Current Biology, Vol. 14, 131–137, January 20, 2004, ©2004 Elsevier Science Ltd. All rights reserved. DOI 10.1016/j.cub.2003.12.058

The Vertebrate Ndc80 Complex Contains Spc24 and Spc25 Homologs, which Are Required to Establish and Maintain Kinetochore-Microtubule Attachment

Mark L. McCleland,[1] Marko J. Kallio,[2] Gregory A. Barrett-Wilt,[3] Cortney A. Kestner,[1] Jeffrey Shabanowitz,[3] Donald F. Hunt,[3,4] Gary J. Gorbsky,[2] and P. Todd Stukenberg[1,*]

[1]Department of Biochemistry and Molecular Genetics
University of Virginia Medical School
Charlottesville, Virginia 22908

[2]Molecular and Cell Biology Research Program
Oklahoma Medical Research Foundation
Oklahoma City, Oklahoma 73104

[3]Department of Chemistry

[4]Department of Pathology
University of Virginia Medical School
Charlottesville, Virginia 22908

Summary

How kinetochores bind to microtubules and move on the mitotic spindle remain unanswered questions. Multiple systems have implicated the Ndc80/Hec1 (Ndc80) kinetochore complex in kinetochore-microtubule interaction and spindle checkpoint activity [1–12]. In budding yeast, Ndc80 copurifies with three additional interacting proteins: Nuf2, Spc24, and Spc25 [4, 5]. Although functional vertebrate homologs of Ndc80 and Nuf2 exist, extensive sequence similarity searches have not uncovered homologs of Spc24 and Spc25. We have purified the xNdc80 complex to homogeneity from *Xenopus* egg extracts and identified two novel interacting proteins. Although the sequences have greatly diverged, we have concluded that these are the functional homologs of the yeast Spc24 and Spc25 proteins based on limited sequence similarity, common coiled-coil domains, kinetochore localization, similar phenotypes, and copurification with xNdc80 and xNuf2. Using both RNAi and antibody injection experiments, we have extended previous characterization of the complex and found that Spc24 and Spc25 are required not only to establish, but also to maintain kinetochore-microtubule attachments and metaphase alignment. In addition, we show that Spc24 and Spc25 are required for chromosomal movement to the spindle poles in anaphase.

Results and Discussion

We purified native xNdc80 complex from *Xenopus* mitotic egg lysates. The complex was followed by immunoblots using antibodies against both xNdc80 and xNuf2 over Heparin-Agarose, Mono-Q, and Superose 6 columns and, finally, affinity purified with anti-xNdc80 antibodies (Figure S1A). Acid elutions from anti-xNdc80 beads contained four stoichiometric proteins located at 75, 55, 27, and 25 kDa that were specific to the anti-xNdc80 immunoprecipitation (Figure 1A). The protein bands at 75 and 55 kDa were identified by immunoblot and mass spectrometry as xNdc80 and xNuf2, respectively. p25 and p27 were identified by mass spectrometry as novel proteins encoded by *Xenopus* EST BU901801 and *Xenopus* EST BU906954, respectively. p25 encodes a 200 amino acid protein with a predicted molecular weight of 23 kDa, and p27 encodes a 229 amino acid protein with a predicted molecular weight of 27 kDa.

Homologs of both novel genes exist in human and mouse genomes, and p27 also shares significant homology to hypothetical protein NP_588208 from *S. pombe* (E value = 1e-08). The *S. pombe* p27 protein sequence was used as a query to BLAST search the *S. kluyveri* genome. The highest scoring sequence was then used to query the *S. castellii* genome, and this procedure was successively repeated against the *S. bayanus*, *S. mikatae*, and *S. cerevisiae* yeast genomes. The highest scoring sequence in *S. cerevisiae* was Spc25 (data not shown). Likewise, the *Xenopus* p25 sequence shares homology to *S. pombe* Spc24, albeit with much weaker homology (E value = 2.4). Similar to that reported for budding yeast Spc24 and Spc25, all metazoan homologs of p25 and p27 contain amino-terminal coiled-coil domains (Figures S1C and S1D; [13]). Due to the copurification of p25 and p27 with xNdc80 and xNuf2, sequence similarity to yeast Spc24 and Spc25, and conserved amino-terminal coiled-coil domains, we have designated these newly identified p25 and p27 proteins as xSpc24 and xSpc25, respectively.

We cloned *xspc24* and *xspc25* and their human homologs (*hspc24* and *hspc25*) and generated antibodies to each protein. Affinity purified anti-xSpc24 and anti-xSpc25 antibodies recognize a single protein at 24 and 26 kDa in both *Xenopus* interphase egg extract (Figure 1B) and *Xenopus* S3 cell lysate (data not shown). Likewise, affinity-purified anti-hSpc24 and anti-hSpc25 antibodies recognize a single protein at 24 and 26 kDa in both DLD-1 (Figure 1B) and HeLa cell lysates (data not shown).

Each complex member was immunoprecipitated from *Xenopus* egg extract, and the resulting precipitates were immunoblotted for each of the other proteins (Figure 1D). xNdc80, xNuf2, xSpc24, and xSpc25 were all found in anti-xNdc80, anti-xNuf2, anti-xSpc24, or anti-xSpc25 immunoprecipitates, respectively. Examination of the supernatants after immunoprecipitation indicated that depletion with either anti-xNdc80 or anti-xSpc25 antibodies also depleted xNdc80, xNuf2, xSpc24, and xSpc25 from the extract (Figure 1D). This suggests that the majority of xNdc80, xNuf2, xSpc24, and xSpc25 proteins are tightly associated in one complex. In addition, the native molecular weight of the complex was determined to be 190 kDa, suggesting that the Ndc80 complex contains one subunit of each of the four proteins (data not shown; [11]).

We performed indirect immunofluorescence with anti-Spc24 and anti-Spc25 antibodies in asynchronously

*Correspondence: pts7h@virginia.edu

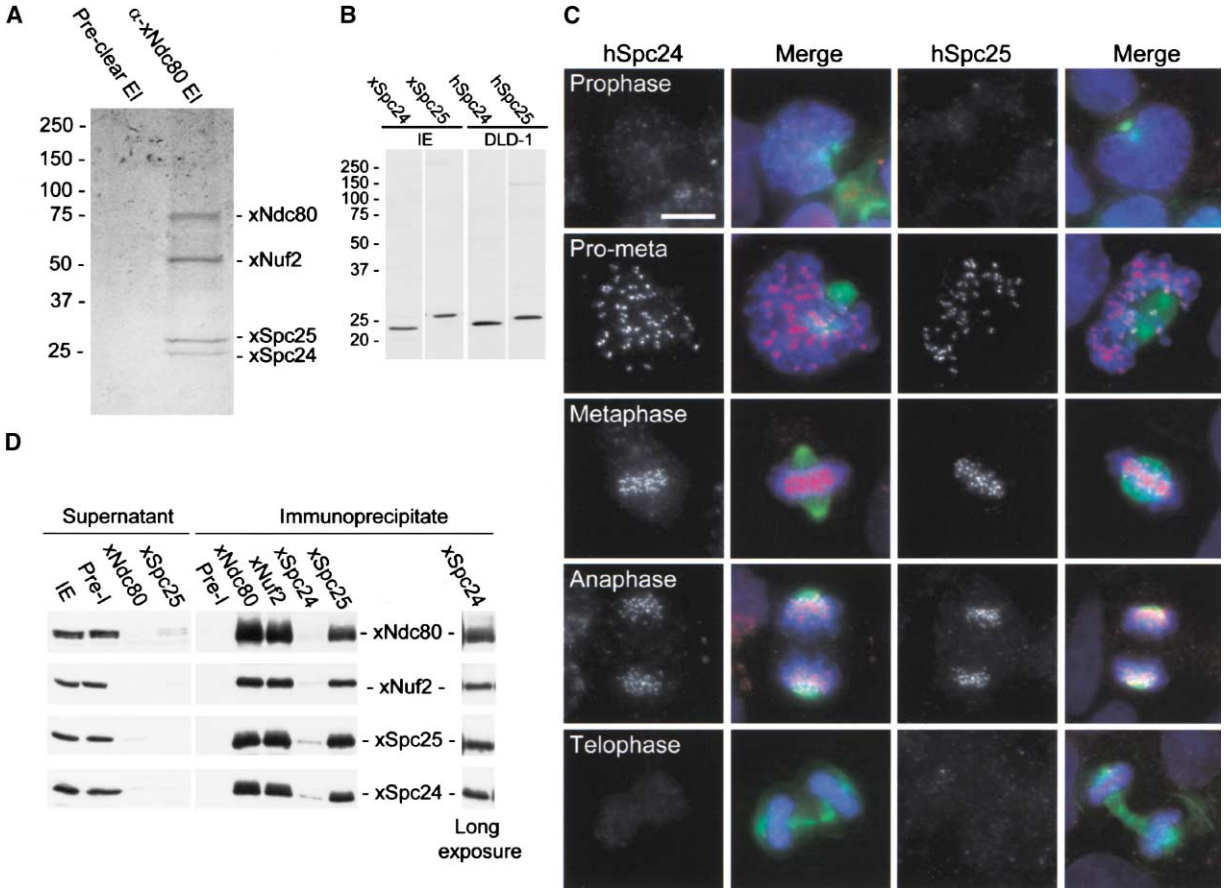

Figure 1. xSpc24 and xSpc25 Form a Complex with xNdc80 and xNuf2 In Vivo and Localize to Kinetochores from Prometaphase through Anaphase

(A) Purification of the xNdc80 complex. *Xenopus* mitotic egg extract was fractionated sequentially over a Heparin-Agarose column, a Mono-Q column, and a Superose 6 gel-filtration column. Fractions from the Superose 6 column were precleared with control rabbit IgG beads prior to immunoprecipitation with anti-xNdc80 beads. Elutions from the xNdc80 complex were precipitated and run on a 4%–20% SDS-PAGE gel. Coomassie-stained proteins were excised from the gel, in gel trypsin digested, and identified by mass spectrometry.

(B) Characterization of polyclonal antibodies generated against xSpc24, xSpc25, hSpc24, and hSpc25. Affinity-purified anti-xSpc24 and anti-xSpc25 antibodies recognize a single ~24 and ~26 kDa protein in *Xenopus* interphase egg extract (IE), respectively. Likewise, affinity-purified anti-hSpc24 and anti-hSpc25 antibodies recognize a single ~24 and ~26 kDa protein in DLD-1 cell lysates (DLD-1).

(C) hSpc24 and hSpc25 are associated with the kinetochore from prometaphase through anaphase. Cycling DLD-1 cells were fixed and stained with mouse anti-tubulin antibody (green) and either anti-hSpc24 or anti-hSpc25 antibody (red), followed by the appropriate secondary antibodies. DNA was visualized by staining with Hoechst 33342 (blue). Cells at each stage of the cell cycle are displayed. Bar, 10 μm.

(D) Coimmunoprecipitation of xSpc24, xSpc25, xNuf2, and xNdc80 from *Xenopus* egg extracts. xNdc80, xNuf2, xSpc24, and xSpc25 were individually immunoprecipitated from *Xenopus* interphase egg extract (IE). The resulting supernatants and precipitates were immunoblotted for xNdc80, xNuf2, xSpc24, and xSpc25. A longer exposure of the xSpc24 immunoprecipitate was required to visualize all four proteins. Preimmune (Pre-I) sera controls did not precipitate any of the four proteins.

growing *Xenopus* S3 cells (data not shown) and human DLD-1 cells (Figure 1C). Both Spc24 and Spc25 associated with kinetochores from prometaphase through anaphase. Kinetochore localization was confirmed by costaining with anti-centromere antigen antibodies (data not shown). The level of either protein at the kinetochore did not significantly change from prometaphase through anaphase. This mitotic localization is identical to that of all metazoan Ndc80 and Nuf2 homologs [14].

HeLa cells were transfected with small interfering RNA (siRNA) duplexes targeted against hSpc24 or hSpc25 and analyzed 26, 50, and 74 hr posttransfection. hSpc24 and hSpc25 protein levels were reduced ~80% 50 hr posttransfection in cells treated with hSpc24 or hSpc25 siRNA duplexes (Figure 2A). Depletion of either hSpc24 or hSpc25 by RNAi also significantly decreased the protein levels of hSpc25 or hSpc24, respectively. Most mitotic cells in the transfected population exhibited hSpc24 or hSpc25 staining below the level of detection by immunofluorescence microscopy (Figure 2D).

Cells transfected with hSpc24 or hSpc25 siRNA duplexes began to accumulate in mitosis by 26 hr posttransfection, and approximately 20% of the cells were in mitosis by 50 hr (Figure 2B). Cells transfected with a control siRNA duplex maintained a mitotic index of 4% through 74 hr. It has been reported in the Nuf2 and Ndc80 knockdown experiments that cells undergo cell death following an 8 hr prometaphase arrest [10, 12]. Similarly, most cells transfected with siRNA duplexes against hSpc24 or hSpc25 had died by 74 hr (data not

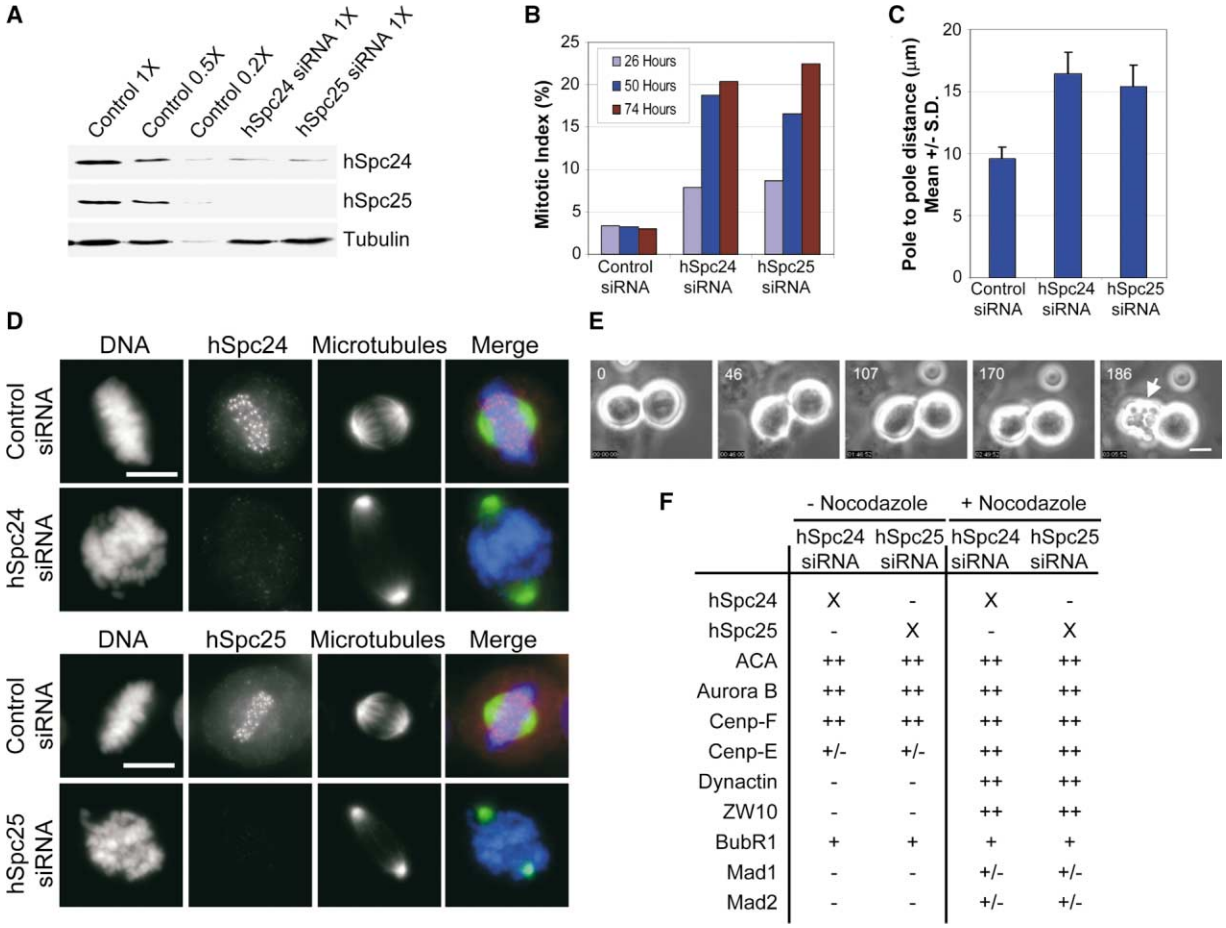

F

	- Nocodazole		+ Nocodazole	
	hSpc24 siRNA	hSpc25 siRNA	hSpc24 siRNA	hSpc25 siRNA
hSpc24	X	-	X	-
hSpc25	-	X	-	X
ACA	++	++	++	++
Aurora B	++	++	++	++
Cenp-F	++	++	++	++
Cenp-E	+/-	+/-	++	++
Dynactin	-	-	++	++
ZW10	-	-	++	++
BubR1	+	+	+	+
Mad1	-	-	+/-	+/-
Mad2	-	-	+/-	+/-

Figure 2. hSpc24 and hSpc25 Knockdown Cells Arrest in Mitosis Exhibiting Defects in Chromosome Alignment Followed by Cell Death

(A) Reduction of hSpc24 and hSpc25 protein levels after siRNA transfection. HeLa cells were transfected with a control, hSpc24, or hSpc25 siRNA duplex and harvested 50 hr posttransfection for protein knockdown analysis by immunoblot. Control lysate was serially diluted and used to estimate the level of protein knockdown in the hSpc24 and hSpc25 siRNA transfections. Tubulin serves as a gel loading control. Hec1 and Nuf2 levels were significantly reduced in some, but not all, experiments after siRNA removal of Spc24 and Spc25 (data not shown).

(B) Knockdown of hSpc24 or hSpc25 results in a mitotic arrest. HeLa cells were transfected with control, hSpc24, or hSpc25 siRNA duplex, and the mitotic index was measured at 26, 50, and 74 hr posttransfection. The mitotic index is displayed as the percentage of mitotic cells in the population.

(C and D) In (C), knockdown of hSpc24 or hSpc25 results in an increased spindle pole-to-pole distance. Fixed cells from (D) were used to measure spindle pole-to-pole distances. Error bars represent standard deviation. (D) Chromosomes fail to congress after knockdown of hSpc24 or hSpc25. Fifty hours posttransfection, cells were fixed and stained with anti-tubulin (green) and either hSpc24 or hSpc25 antibodies (red). DNA was visualized by staining with Hoechst 33342 (blue). Bar, 10 μm.

(E) hSpc25 RNAi induces M phase arrest and cell death. HeLa cells were transfected with hSpc25 siRNA duplex and filmed 48 hr posttransfection for ~4 hr. Two cells were filmed that were arrested in mitosis at the beginning of the time-lapse session. One of the two cells (arrow) underwent cell death without exiting mitosis. Numbers show the minutes from the beginning of the time-lapse session. The still images correspond to Movie 1. Bar, 10 μm.

(F) Summary of kinetochore structure in hSpc24 or hSpc25 knocked down cells. Forty-eight hours posttransfection, RNAi-treated cells were incubated for 2 hr in the presence or absence of nocodazole. Cells were subsequently fixed and stained for the indicated kinetochore proteins. 50 cells were counted to determine the status of each kinetochore protein. All cells were costained with anti-centromere antibody (ACA) to identify the location of kinetochores (data not shown). X, removal of target protein; ++, kinetochore localization with levels equivalent to control cells; +, kinetochore localization with reduced levels as compared to control cells; +/−, kinetochore staining varied from reduced to below the limit of detection; −, loss of kinetochore association.

shown). We filmed hSpc24 and hSpc25 knocked down cells over a period of 4 hr. Mitotic cells remained arrested for at least 3 hr, after which their cell membranes underwent the intense blebbing characteristic of cell death (Figure 2E and Movie 1). We conclude that RNAi of hSpc24 and hSpc25 generates mitotic arrest followed by cell death.

To determine if knockdown of hSpc24 or hSpc25 also caused defects in chromosome congression, HeLa cells were transfected with a control, hSpc24, or hSpc25 siRNA duplex, fixed 50 hr posttransfection, and examined by immunofluorescence microscopy. Control metaphase cells exhibited chromosomes with tight metaphase alignment and robust microtubule bundles emanating from each spindle pole that were embedded in hSpc24 and hSpc25 staining on aligned chromosomes (Figure 2D). In contrast, the majority of cells knocked down for hSpc24 or hSpc25 displayed chromo-

somes distributed over the mitotic spindle and lacked detectable kinetochore microtubules (Figure 2D). Furthermore, the spindle pole-to-pole distance was approximately 65% longer in both the hSpc24 (16.46 ± 1.71 μM, n = 21) and hSpc25 (15.42 ± 1.73 μM, n = 23) siRNA-treated cells compared to control metaphase spindles (9.6 μM ± 0.9 μM, n = 21; Figure 2C). We conclude that hSpc24 or hSpc25 are required for normal kinetochore function since depleted cells are unable to congress chromosomes, form normal kinetochore-microtubule attachments, or generate tension between spindle poles.

To determine the structure of the kinetochore after depleting hSpc24 and hSpc25, RNAi-treated cells were incubated 48 hr posttransfection in the presence or absence of nocodazole for 2 hr and then subsequently stained for numerous kinetochore proteins. Consistent with the immunoblot analysis, both hSpc24 and hSpc25 failed to associate with kinetochores after hSpc24 or hSpc25 RNAi (Figures 2F and S2). In the presence and absence of nocodazole, antibodies to Aurora B, ACA, and Cenp-F labeled kinetochores with the same intensity as control-transfected cells, suggesting that inner kinetochore structure was not disrupted (Figures 2F and S2). Cenp-E levels varied on a cell-to-cell basis from approximately 25% (40% of both the hSpc24 and hSpc25 knockdown cells; n = 50) to below the level of detection (60% of cells; n = 50). Since antibodies to Cenp-E, hSpc24, and hSpc25 are all of the same species, we were unable to label Cenp-E and hSpc24/hSpc25 in the same cells. Thus variability in Cenp-E levels may result from a corresponding variability in siRNA-mediated knockdown of hSpc24 and hSpc25. Surprisingly, treatment with nocodazole restored Cenp-E levels to that of control cells. Dynactin and Zw10 were absent from kinetochores; however, treatment with nocodazole also restored their association. This suggests that in cells lacking hSpc24 and hSpc25, the outer kinetochore proteins associate with kinetochores but are disassembled in a microtubule-dependent manner.

Similar to knockdown of Hec1 and Nuf2 [9, 10, 12], the checkpoint proteins Mad1 and Mad2 were not detectable at kinetochores after knockdown of hSpc24 and hSpc25. In addition, treating cells with nocodazole only slightly restored the kinetochore association of Mad1 and Mad2 (Figures 2F and S2). The cells shown in Figure S2B for Mad2 staining is the strongest recovery we witnessed (38% of Spc24 knockdown cells and 44% of Spc25 knockdown cells; n = 50), and most cells displayed staining below the level of detection. Similar results were found for Mad1 staining. Since the antibodies to hSpc24 and hSpc25 are of the same species as Mad1 and Mad2 antibodies, we were not able to label for hSpc24/hSpc25 and Mad1/Mad2 in the same cells. Thus the variability in Mad1 and Mad2 levels may result from a corresponding variability in siRNA-mediated knockdown of hSpc24 and hSpc25. The BubR1 checkpoint protein was also reduced on kinetochores after hSpc24 or hSpc25 knockdown, and its levels were not restored by nocodazole treatment.

To study the immediate consequences of inhibiting Spc24 and Spc25 in living cells, we microinjected antibodies into *Xenopus* S3 cells and followed them by time-lapse microscopy. Prophase (Movies 2 and 3) or prometaphase (data not shown) cells injected with xSpc24 (n = 25) or xSpc25 (n = 25) antibodies never achieved metaphase alignment; however, chromosomes randomly oscillated parallel to the orientation of the mitotic spindle, suggesting that kinetochores could still interact with microtubules. Within 45 min after injection, unaligned chromatids separated and the cell exited mitosis, implying that the spindle checkpoint was abrogated. Sister chromatids appeared to lose all connections with microtubules at the onset of anaphase as chromosomes displayed no oscillations or movements toward the spindle poles. Chromosomes remained near the spindle equator, decondensed, and the cytokinetic furrow cut through the mass of chromatids (Movies 2 and 3). Control *Xenopus* S3 cells injected with nonimmune rabbit IgG (n = 20) progressed normally through mitosis (data not shown). We conclude that xSpc24 and xSpc25 are required for chromosome congression in prometaphase and movements to the poles in anaphase.

Defects in the ability to establish kinetochore-microtubule attachment [10] may be a result of improper mitotic entry, defects in kinetochore or spindle assembly, altered microtubule dynamics, the inability to insert microtubules into the kinetochore, or the failure to stabilize kinetochore-microtubule attachments. Therefore, to determine if xSpc24 and xSpc25 are only required during initial kinetochore-microtubule capture or whether they are additionally required for the maintenance of mature kinetochore-microtubule attachments, we allowed cells to progress normally to metaphase in the presence of MG132, a proteasome inhibitor. Then xSpc24 and xSpc25 activity was subsequently inhibited by antibody injection. In the majority of metaphase cells injected with anti-xSpc24 (30 of 40 cells) or anti-xSpc25 (65 of 77 cells) antibodies, chromosomes were unable to maintain metaphase alignment and underwent bidirectional oscillations along the spindle axis (Figure 3B and Movie 4). Metaphase *Xenopus* S3 cells injected with nonimmune rabbit IgG (n = 20) remained at metaphase with their chromosomes tightly aligned at the metaphase plate (Figure 3A and Movie 5). These data suggest that Spc24 and Spc25 are required throughout mitosis to maintain proper kinetochore-microtubule attachment.

The loss of chromosome congression in cells where xSpc24 and xSpc25 were inhibited was accompanied by alterations in kinetochore-microtubule attachments. We injected metaphase *Xenopus* S3 cells with nonimmune rabbit IgG, anti-xSpc24, or anti-xSpc25 antibodies in the presence of MG132. After 90 min, cells were fixed and immunolabeled with anti-tubulin antibody. All control cells (n = 20) displayed a normal bipolar spindle with kinetochore-microtubules connecting aligned chromosomes to spindle poles (Figure 3C). In cells injected with anti-xSpc24 or anti-xSpc25 antibodies, normal kinetochore-microtubule bundles were not seen. Instead long, continuous microtubule bundles appeared to extend uninterrupted from spindle pole to pole (Figure 3C). These microtubule bundles were resistant to detergent lysis in cold calcium buffer, which disassembles most microtubules, but preserves kinetochore-microtubule bundles and interdigitating pole-to-pole microtubule bundles (Figure 4A). In addition, a minority of cells in-

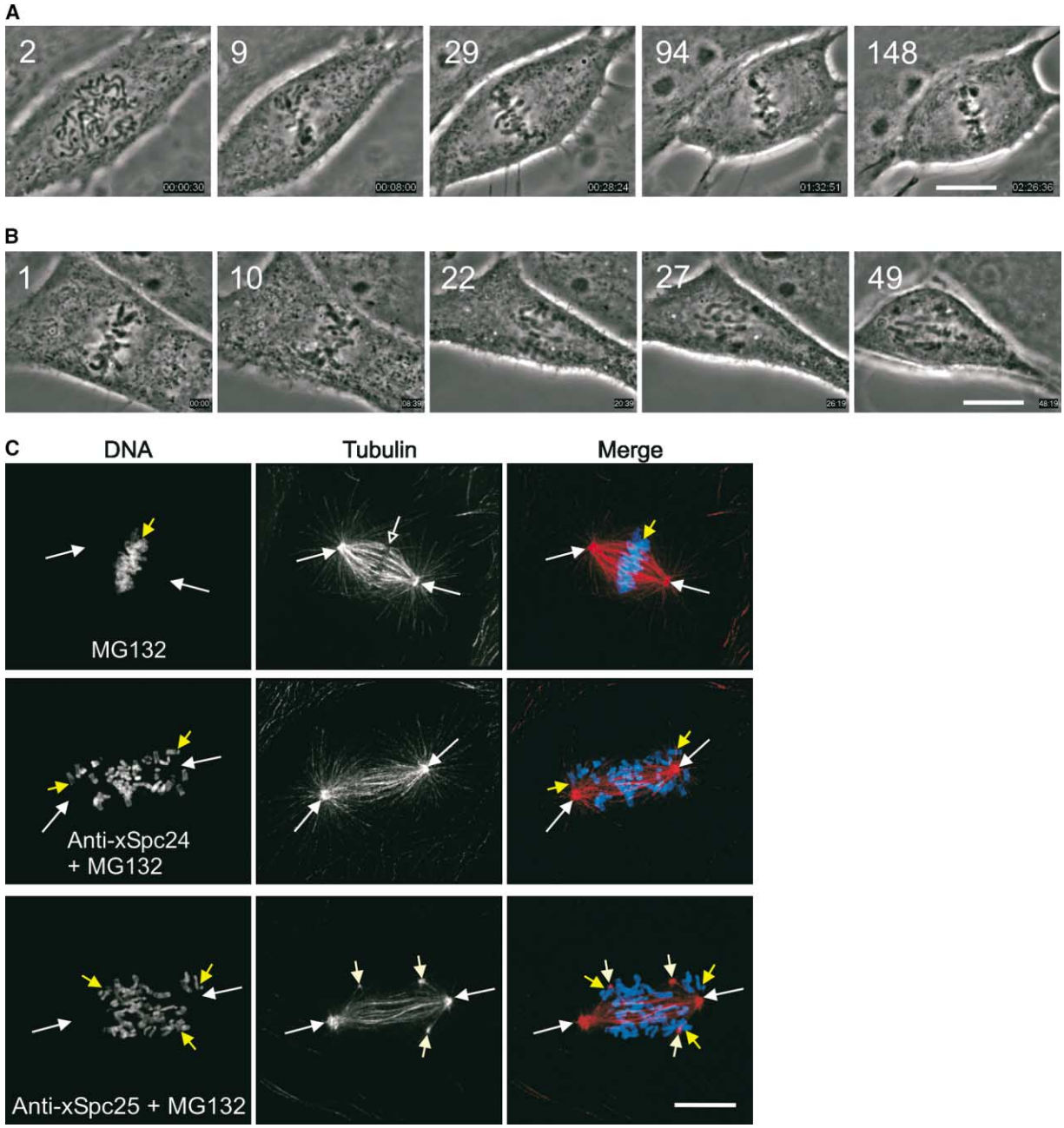

Figure 3. Spc24 and Spc25 Are Required to Maintain Metaphase Chromosome Alignment

(A) A control *Xenopus* S3 cell was injected with nonimmune rabbit IgG at late prophase in the presence of MG132. All chromosomes aligned to the spindle equator where they exhibited normal oscillatory movements. The still frames correspond to Movie 4.

(B) A metaphase-arrested *Xenopus* S3 cell was injected with anti-xSpc25 antibody. Most chromosomes lost alignment within 25 min after the antibody injection and distributed between the spindle poles. The numbers denote time in minutes after the antibody injection. The still frames correspond to Movie 5.

(C) Metaphase *Xenopus* S3 cells were injected with anti-xSpc24, anti-xSpc25, or control rabbit IgG antibodies; incubated for 90 min in MG132; fixed; and processed for immunofluorescence. Top shows a control cell with a bipolar spindle (white arrows, location of the spindle poles) and all the chromosomes aligned at the metaphase plate (yellow arrowheads). The open white arrow denotes the gap between the bipolar kinetochore-microtubule bundles at the spindle equator. Middle and bottom show anti-xSpc24 and anti-xSpc25 antibody-injected cells, respectively. Note the elongated spindles that lack kinetochore-microtubule fibers and the chromosomes that lost metaphase alignment (yellow arrowheads) and relocated near the spindle poles (white arrows) or to extrasatellite poles (white arrowheads). Bars, 10 μm.

jected with anti-xSpc24 (8 out of 40 cells) or with anti-xSpc25 (17 out of 77 cells) antibodies developed satellite spindle pole foci.

The average spindle pole-to-pole distance in cells injected with anti-xSpc25 antibody was significantly longer (18.1 ± 1.6 μm), compared to control metaphase

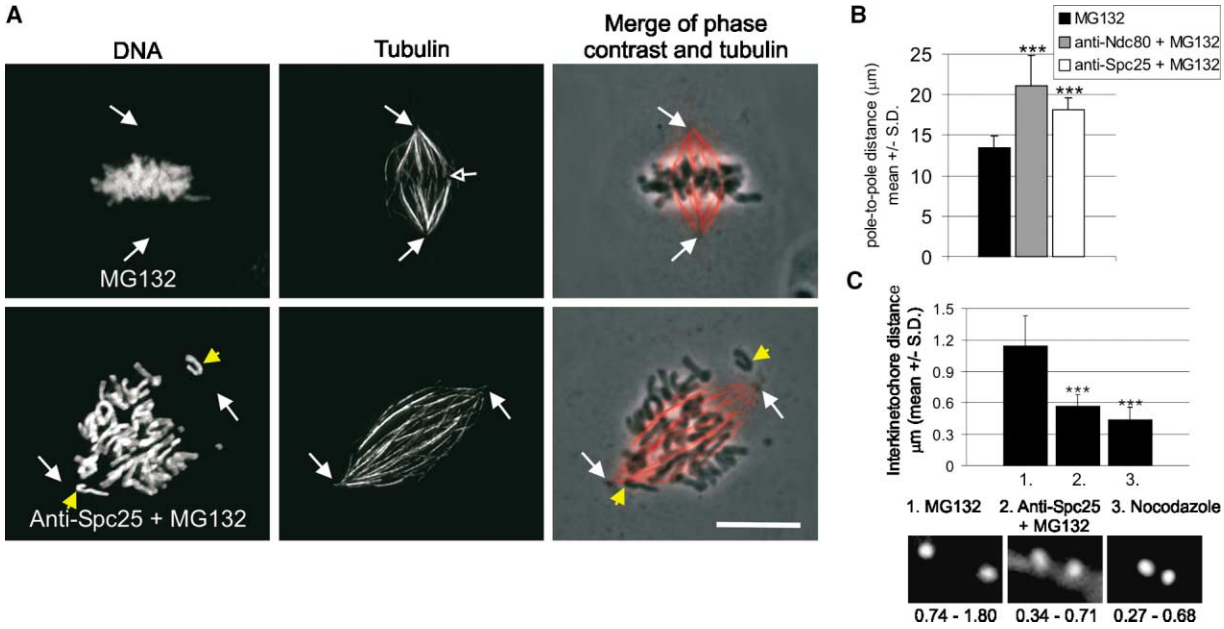

Figure 4. Cells Injected with Anti-xSpc24 or Anti-xSpc25 Antibodies Abolish Kinetochore Microtubules and Display Elongated Spindles and Reduced Interkinetochore Tension

(A) Metaphase *Xenopus* S3 cells were injected with control rabbit IgG (top) or anti-xSpc25 antibodies (bottom), incubated for 90 min in MG132, lysed with cold calcium buffer, fixed, and processed for immunofluorescence. All chromosomes in the control cells remained aligned at the metaphase plate and were attached to kinetochore-microtubule fibers (open white arrowhead). White arrows indicate the location of the spindle poles. In the anti-xSpc25 antibody-injected cell, kinetochore-microtubule fibers were replaced by stable pole-to-pole microtubule bundles. Note that there are many unaligned chromosomes (yellow arrowheads), and some have moved to the spindle poles (white arrows). Bar, 10 μm.

(B) Average pole-to-pole distance in noninjected, anti-xNdc80, and anti-xSpc25 antibody-injected *Xenopus* S3 cells. The cells (n = 20 per group) were injected at metaphase in MG132, incubated for 90 min, fixed, and processed for immunofluorescence. Asterisks denote a statistically significant difference between the controls and the antibody injected cell populations.

(C) Average interkinetochore distance in cells treated with MG132, nocodazole, or injected with anti-xSpc25 antibodies in MG132. The interkinetochore distance was measured from ten sister kinetochore pairs in three cells (n = 30) per group. Asterisks denote a statistically shorter interkinetochore distance compared to metaphase cells in MG132. Inset micrographs show examples of the interkinetochore distance from each group. Numbers denote the range of the interkinetochore distances.

IgG-injected cells (13.5 ± 1.5 μm; Figure 4B). This is similar to results found after RNAi of hSpc24 and hSpc25 or after injection of anti-xNdc80 antibodies (21.1 ± 3.8 μm). Interkinetochore distance in control cells treated with MG132 (to measure maximal metaphase tension) or nocodazole (to remove tension) was 1.15 ± 0.29 μm and 0.44 ± 0.12 μm, respectively. The interkinetochore distance in cells injected with anti-xSpc25 antibody was 0.57 ± 0.11 μm (Figure 4C). These results show that cells lacking xSpc25 function fail to maintain either interkinetochore or spindle pole-to-pole tension and provide further evidence that kinetochores do not properly bind the mitotic spindle.

We have purified the *Xenopus* Ndc80 complex and identified functional homologs of Spc24 and Spc25. Identification of vertebrate Spc24 and Spc25 homologs suggests that although many protein sequences may have greatly diverged, overall architecture and principal kinetochore function is conserved from budding yeast to humans. We and others have previously shown that the loss of Ndc80 complex function results in a defect in chromosome congression and in the formation of interkinetochore tension and mature kinetochore-microtubule attachments [9–12]. We have extended this by demonstrating that the outer kinetochore was disassembled in a microtubule-dependent manner and that congression of chromosomes to the metaphase plate and anaphase chromosome movements are abrogated in cells depleted of Spc24 and Spc25 function. We also conclude that Spc24 and Spc25 are not dispensable after the formation of mature kinetochore-microtubule attachments. Normally, kinetochore attachments to microtubules appear to progress from an initial lateral attachment to a mature end-on attachment. We propose that the Ndc80 complex inhibits the release of the outer kinetochore components or is critical for the maturation into end-on microtubule binding. We suggest that the Ndc80 complex, required for chromosome congression and anaphase chromosome movement, is an excellent candidate to mediate the interaction of microtubule plus ends with kinetochore function.

Supplemental Data

Supplemental figures, movies, and experimental procedures describing the complex purification, kinetochore assembly, and antibody injections are available at http://www.current-biology.com/cgi/content/full/14/2/131/DC1/.

Acknowledgments

We would like to thank Doug DeSimone for the *Xenopus* S3 cells; John Daum and Dan Burke for helpful comments; Jennifer DeLuca

and Ted Salmon for antibodies and sharing unpublished data; Tim Yen for antibodies; and the members of the Burke, Gorbsky, and Stukenberg labs for support. Dan Burke was especially helpful by performing the yeast database searches. G.A.B., J.S., and D.F.H. are supported by the US Public Health Service Grant (GM37537). M.J.K. and G.J.G. are supported by a grant from the National Institutes of Health (GM50412). M.L.M., C.A.K., and P.T.S. are supported by the National Institutes of Health (GM63045) and by the Pew Charitable Trust.

Received: October 3, 2003
Revised: December 4, 2003
Accepted: December 5, 2003
Published: January 20, 2004

References

1. Osborne, M.A., Schlenstedt, G., Jinks, T., and Silver, P.A. (1994). Nuf2, a spindle pole body-associated protein required for nuclear division in yeast. J. Cell Biol. *125*, 853–866.
2. Chen, Y., Riley, D.J., Chen, P.L., and Lee, W.H. (1997). HEC, a novel nuclear protein rich in leucine heptad repeats specifically involved in mitosis. Mol. Cell. Biol. *17*, 6049–6056.
3. Wigge, P.A., Jensen, O.N., Holmes, S., Soues, S., Mann, M., and Kilmartin, J.V. (1998). Analysis of the Saccharomyces spindle pole by matrix-assisted laser desorption/ionization (MALDI) mass spectrometry. J. Cell Biol. *141*, 967–977.
4. Wigge, P.A., and Kilmartin, J.V. (2001). The Ndc80p complex from Saccharomyces cerevisiae contains conserved centromere components and has a function in chromosome segregation. J. Cell Biol. *152*, 349–360.
5. Janke, C., Ortiz, J., Lechner, J., Shevchenko, A., Magiera, M.M., Schramm, C., and Schiebel, E. (2001). The budding yeast proteins Spc24p and Spc25p interact with Ndc80p and Nuf2p at the kinetochore and are important for kinetochore clustering and checkpoint control. EMBO J. *20*, 777–791.
6. Howe, M., McDonald, K.L., Albertson, D.G., and Meyer, B.J. (2001). HIM-10 is required for kinetochore structure and function on Caenorhabditis elegans holocentric chromosomes. J. Cell Biol. *153*, 1227–1238.
7. Nabetani, A., Koujin, T., Tsutsumi, C., Haraguchi, T., and Hiraoka, Y. (2001). A conserved protein, Nuf2, is implicated in connecting the centromere to the spindle during chromosome segregation: a link between the kinetochore function and the spindle checkpoint. Chromosoma *110*, 322–334.
8. He, X., Rines, D.R., Espelin, C.W., and Sorger, P.K. (2001). Molecular analysis of kinetochore-microtubule attachment in budding yeast. Cell *106*, 195–206.
9. Martin-Lluesma, S., Stucke, V.M., and Nigg, E.A. (2002). Role of hec1 in spindle checkpoint signaling and kinetochore recruitment of mad1/mad2. Science *297*, 2267–2270.
10. DeLuca, J.G., Moree, B., Hickey, J.M., Kilmartin, J.V., and Salmon, E.D. (2002). hNuf2 inhibition blocks stable kinetochore-microtubule attachment and induces mitotic cell death in HeLa cells. J. Cell Biol. *159*, 549–555.
11. McCleland, M.L., Gardner, R.D., Kallio, M.J., Daum, J.R., Gorbsky, G.J., Burke, D.J., and Stukenberg, P.T. (2003). The highly conserved Ndc80 complex is required for kinetochore assembly, chromosome congression, and spindle checkpoint activity. Genes Dev. *17*, 101–114.
12. Hori, T., Haraguchi, T., Hiraoka, Y., Kimura, H., and Fukagawa, T. (2003). Dynamic behavior of Nuf2-Hec1 complex that localizes to the centrosome and centromere and is essential for mitotic progression in vertebrate cells. J. Cell Sci. *116*, 3347–3362.
13. Lupas, A., Van Dyke, M., and Stock, J. (1991). Predicting coiled coils from protein sequences. Science *252*, 1162–1164.
14. Cleveland, D.W., Mao, Y., and Sullivan, K.F. (2003). Centromeres and kinetochores: from epigenetics to mitotic checkpoint signaling. Cell *112*, 407–421.

Accession Numbers

The *xspc24*, *xspc25*, *hspc24*, and *hspc25* gene sequences were deposited into GenBank (xSpc24-AY456385, xSpc25-AY456386, hSpc24-AY456387, and hSpc25-AY456388, respectively).